RESEARCH ARTICLE | AUGUST 06 2015

Effect of channel thickness, electrolyte ions, and dissolved oxygen on the performance of organic electrochemical transistors

Prajwal Kumar; Zhihui Yi; Shiming Zhang; Arvindh Sekar ; Francesca Soavi; Fabio Cicoira

Appl. Phys. Lett. 107, 053303 (2015)
https://doi.org/10.1063/1.4927595

Effect of channel thickness, electrolyte ions, and dissolved oxygen on the performance of organic electrochemical transistors

Prajwal Kumar,[1] Zhihui Yi,[1] Shiming Zhang,[1] Arvindh Sekar,[1] Francesca Soavi,[2] and Fabio Cicoira[1,a)]
[1]Department of Chemical Engineering, Polytechnique Montréal, C.P. 6079, Succ. Centre Ville, Montréal, QC H3C 3A7, Canada
[2]Department of Chemistry "Giacomo Ciamician," Alma Mater Studiorum - Università di Bologna, Via Selmi, 2, Bologna 40126, Italy

(Received 13 May 2015; accepted 17 July 2015; published online 6 August 2015)

We investigated the device characteristics of organic electrochemical transistors based on thin films of poly(3,4-ethylenedioxythiophene) doped with poly(styrene-sulfonate). We employed various channel thicknesses and two different electrolytes: the micelle forming surfactant cetyltrimethyl ammonium bromide (CTAB) and NaCl. The highest ON/OFF ratios were achieved at low film thicknesses using CTAB as the electrolyte. Cyclic voltammetry suggests that a redox reaction between oxygen dissolved in the electrolytes and PEDOT:PSS leads to low ON/OFF ratios when NaCl is used as the electrolyte. Electrochemical impedance spectroscopy reveals that doping/dedoping of the channel becomes slower at high film thickness and in the presence of bulky ions. [http://dx.doi.org/10.1063/1.4927595]

Organic conducting polymers lay the foundation for organic bioelectronics.[1–7] Poly(3,4-ethylenedioxythiophene) doped with poly(styrene-sulfonate) (PEDOT:PSS) is a well known highly conducting and optically transparent polymer.[8,9] Organic electrochemical transistors (OECTs) based on PEDOT:PSS are exploited in bioelectronics and sensing.[3,10–12] OECTs consist of a conducting polymer channel, connected to source and drain electrodes that are in ionic contact with a gate electrode via an electrolyte solution. OECTs based on PEDOT:PSS work in depletion mode: a hole source-drain current (I_{ds}) flows upon application of a drain-source voltage (V_{ds}). When a positive gate-source voltage (V_{gs}) is applied, electrolyte cations enter the channel and dedope it, thus leading to a decrease of I_{ds}. An important figure of merit OECTs is the current modulation, typically expressed in terms of ON/OFF ratio, which depends on processing and composition of the conducting polymer channel,[13] device geometry,[14–17] gate material,[18,19] and nature of the electrolyte.[20–22] OECT performance is also affected by the thickness of the conducting polymer channel. As current modulation relies on redox processes, which involve exchange of ions between the electrolyte and the polymer film, the entire film volume is relevant for charge transport. This working mechanism differs from that of organic field effect transistors, where only the very first few monolayers at the gate dielectric/channel interface are relevant for charge carrier transport.[23] Malliaras *et al.* have recently demonstrated that the transconductance (dI_{ds}/dV_{gs}) and the capacitance of PEDOT:PSS OECTs depend on channel thickness and aspect ratio.[24,25]

Here, we investigate the effect of the PEDOT:PSS channel thickness on OECT modulation using two different electrolytes: the cationic surfactant hexadecyltrimethylammonium bromide, also known as cetyltrimethyl ammonium bromide (CTAB) and NaCl. CTAB, beyond its critical micelle concentration (CMC), is known to lead to high current modulation in OECTs and it is therefore a model system to study the doping/dedoping process in OECTs.[20] We employed cyclic voltammetry (CV) and electrochemical impedance spectroscopy (EIS) to gain insight into the impact of channel thickness and nature of the electrolyte on device performance.

The OECT's PEDOT:PSS channels were patterned on a glass substrates using a procedure previously published.[14] The effective channel dimensions (geometric area of about 12 mm^2) were defined by the contact region between the film and the electrolyte, confined into a cloning cylinder.[18] Films were deposited by spin coating a mixture containing a PEDOT:PSS suspension (Clevios™ PH 1000, Haraeus GmbH, Germany), the conductivity enhancer ethylene glycol (19.7 v/v%), and dodecylbenzenesulfonic acid (DBSA) (0.3 v/v %).[26] Different speeds (500, 1000, 2000, and 4000 rpm for 20 s) were employed to achieve film thicknesses of about 500, 180, 110, and 50 nm, as measured by a Dektak 150 optical profilometer. The electrical conductivity of PEDOT:PSS films was extracted from the sheet resistance, measured by a four-point probe system.[27] Activated carbon (AC) gate electrodes (geometric area about 25 mm^2) were prepared by drop casting a suspension of AC (Picachem BP9, 28 mg ml^{-1}) and Nafion (2.4 mg ml^{-1}) in isopropanol on carbon fiber paper (Spectracarb 2050, 10 mils).[19] Aqueous solutions of 0.01M NaCl and 0.001M CTAB (i.e., above the CMC) were used as the electrolytes. The ionic conductivity of the electrolytes was measured by a Traceable® expanded range conductivity meter. OECT characterization was carried in ambient conditions with an Agilent 2902A source/measure unit controlled via Labview software. Transfer curves were extracted from OECT transient characteristics (I_{ds} versus time) measured at different V_{gs}. CV and EIS were carried out in a three-electrode cell, where a PEDOT:PSS film acted as the working electrode (WE), a Pt foil as the counter electrode (CE), and aqueous Ag/AgCl as

a)E-mail: fabio.cicoira@polymtl.ca

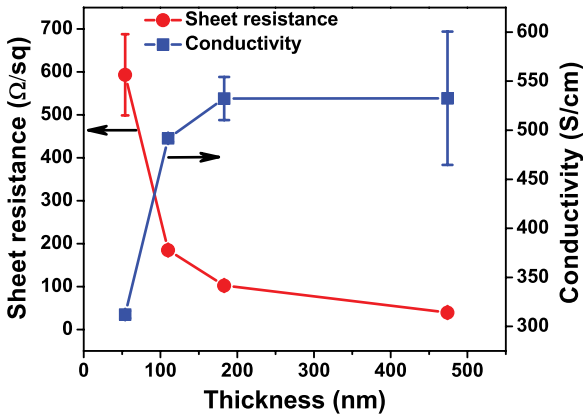

FIG. 1. Sheet resistance (red circles, left y axis) and electrical conductivity (blue stars, right y axis) of PEDOT:PSS films (geometric area of $15 \times 15\,mm^2$) of different thicknesses (~500, 180, 110, and 50 nm). The error bars correspond the standard deviation of four samples.

the reference electrode (RE). The electrolyte solutions were purged with N_2 or air for 1 h prior to measurements and during the CV (at reduced flow to prevent the formation of foam in CTAB). A hollow cylindrical well confined the electrolyte on the WE (over an area of $0.64\,cm^2$).

To highlight the role of channel resistance in OECTs' modulation, we first measured the electrical conductivity of PEDOT:PSS films at four different thicknesses (Figure 1). The conductivity increases from $\sim 300\,S\,cm^{-1}$ to $\sim 450\,S\,cm^{-1}$ as thickness increases from ~50 nm to ~110 nm. Further increase in thickness to ~180 nm and ~500 nm results in a modest increase up to $\sim 500\,S\,cm^{-1}$. This behavior can be tentatively explained with a transition from percolation to bulk-like charge transport occurring upon film thickness increase. This would be an analogy to conduction in two-dimensional materials such as graphene.[28] A percolative behavior is characteristic of sparse networks with limited connectivity and few continuous conductive paths. Thus, we hypothesize that in case of 50 nm thick PEDOT:PSS films, charge carriers are mainly transported in quasi-two dimensional paths between adjacent PEDOT grains, while in thicker films they are transported in three dimensional PEDOT-PEDOT networks.

The transfer characteristics ($-0.4\,V \le V_{gs} \le 0.6\,V$ and $V_{ds} = -0.2\,V$) of OECTs with different channel thicknesses (Figure 2(a) for NaCl electrolyte and Figure 2(b) for CTAB electrolyte) show the typical I_{ds} vs V_{gs} behavior of PEDOT:PSS OECTs and reveal that, at a given V_{gs}, $|I_{ds}|$ increases with increasing channel thickness. This trend confirms that the transport of electronic charge carriers takes place in the entire channel volume.

The ON/OFF ratios (Table I) are significantly higher for devices using the CTAB electrolyte, in agreement with the previously published results.[20] Decreasing the film thickness from ~500 to ~50 nm leads to an increase of the ON/OFF ratio from ~50 to ~220. The same thickness variation leads to minor changes in devices using the NaCl electrolyte. ON/OFF ratios as high as ~1700 (at $V_{ds} = -0.5\,V$ and V_{gs} varying from $-0.8\,V$ to $0.6\,V$) were achieved with OECTs using a 110 nm thick PEDOT:PSS channel and 0.001M CTAB electrolyte (Figure 2(c)). The devices show negligible hysteresis under our measurements conditions (Figure 2(d)).

To further investigate the effects of channel thickness and electrolyte composition on current modulation, we performed CV. Figure 3(a) shows CVs of PEDOT:PSS films in CTAB and NaCl. The potential of the WE was swept from 0 V vs Ag/AgCl towards negative potentials (−1 V vs. Ag/AgCl) and then towards positive potentials (+0.8 V vs. Ag/AgCl) with a scan rate of 5 mV/s. Under N_2 purging, the position of the redox peaks in the two electrolytes does not differ significantly: the typical oxidation wave is observed between −0.4 V and 0.5 V vs. Ag/AgCl and the reduction

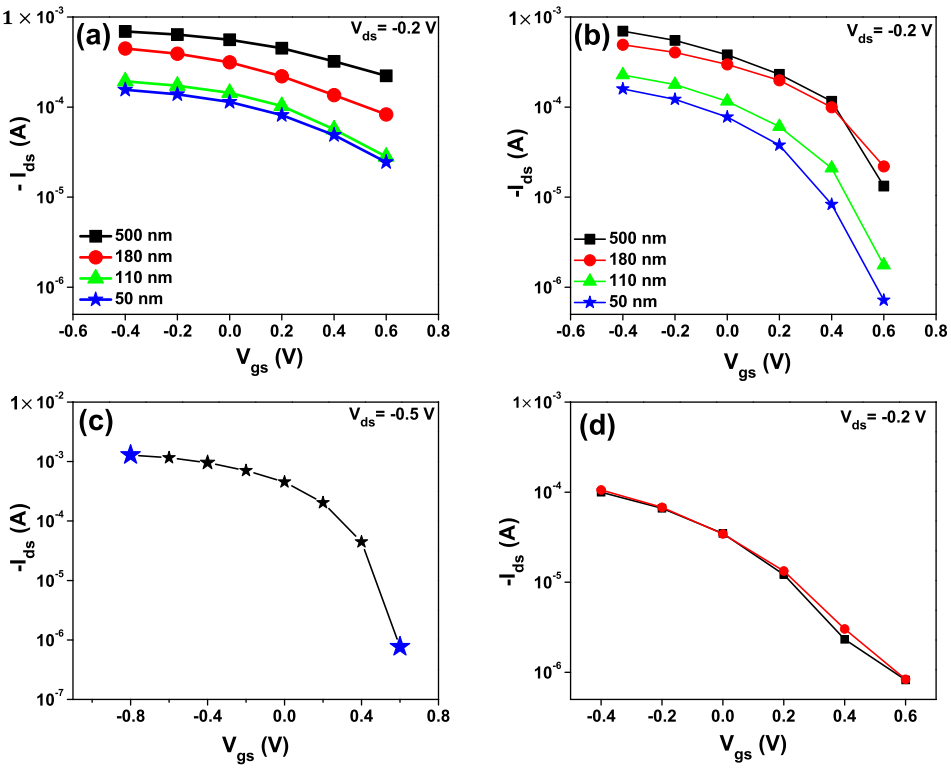

FIG. 2. Transfer characteristics ($-0.4\,V \le V_{gs} \le 0.6\,V$ and $V_{ds} = -0.2\,V$) of PEDOT:PSS OECTs with four different channel thicknesses (~500 nm, 180 nm, 110 nm, and 50 nm) using 0.01M NaCl (a) and 0.001M CTAB (b) as the electrolyte. OECT based on a 110 nm thick PEDOT:PSS film using 0.001M CTAB as the electrolyte, showing a high ON/OFF ratio of ~1700 ($V_{ds} = -0.5\,V$ and V_{gs} varying from $-0.8\,V$ to $0.6\,V$). The blue star represents the ON and OFF currents at $V_{gs} = -0.8$ and $V_{gs} = 0.6\,V$ (c). Hysteresis behavior of an OECT based on a 50 nm thick PEDOT:PSS film. The black curve corresponds to the forward bias (from $V_{gs} = -0.4$ to $V_{gs} = 0.6$ with $V_{ds} = -0.2\,V$) and the red curve to the reverse bias (d).

TABLE I. ON/OFF ratios extracted from transfer characteristics ($-0.4\,V \le V_{gs} \le 0.6\,V$ and $V_{ds} = -0.2\,V$) of PEDOT:PSS OECTs with four different channel thicknesses (~500, 180, 110, and 50 nm) using 0.01M NaCl and 0.001M CTAB as the electrolytes.

	ON/OFF ratio	
Thickness (nm)	NaCl electrolyte	CTAB electrolyte
474 ± 90	~7.0	~50
180 ± 10	~5.5	~180
110 ± 10	~7	~130
55 ± 5	~7	~220

takes place between −0.4 V and −0.8 V vs Ag/AgCl. The voltammograms are more distorted in CTAB, which suggests a slowed down doping/dedoping process with respect to NaCl, likely related to lower ionic conductivity (~0.1 mS/cm for 0.001M CTAB with respect to ~2.0 mS/cm for 0.01M NaCl), slower migration, and higher steric hindrance. Indeed, the diameter of the positively charged CTA^+ micelle is ~1−4 nm (Refs. 19 and 29) and that of Na^+ is ~0.2 nm.

The intensity of the CV current increases with increasing film thickness from ~50 nm to ~500 nm (Figure 3(b)). The amount of charge needed to dedope/dope the films (Q) was calculated by integration of the anodic current over time and the film capacitance was calculated from the slope of Q (during doping) vs electrode potential (Table II). An increase of the film capacitance of about a factor of 6 was found upon a thickness increase from 50 nm to 500 nm. These results, in agreement with recent findings by Malliaras *et al.*,[25] are consistent with the dedoping/doping mechanism of PEDOT:PSS films, which involves incorporation/release of electrolyte cations: the CV current depends on the dedoping/doping charge, in turn related to the amount (thickness) of PEDOT:PSS to be dedoped/doped. The values of the volumetric capacitance are higher in thinner films, which points to a more effective dedoping/doping process at lower thicknesses. Although higher values are found for CTAB, the effect of the electrolyte is rather modest.

As OECTs are mostly operated in ambient conditions, we explored the effect of dissolved oxygen on the redox behavior of PEDOT:PSS films (~50 nm thickness) by carrying out CV under air purging (Figures 3(c) and 3(d), red dotted curves). Voltammograms obtained under air purging indicate an increase of the cathodic current between −0.5 V and −0.8 V vs Ag/AgCl for both electrolytes. This suggests that PEDOT:PSS, once it is electrochemically reduced to the dedoped state, it is readily reoxidized chemically to the doped state by dissolved O_2,[30] with a process similar to that exploited for electrocatalytic oxygen reduction at PEDOT electrodes.[31–35] In OECTs, this effect may hinder the dedoping of PEDOT:PSS that is expected at positive V_{gs}, thus leading to lower ON/OFF ratios. The cathodic current is higher in NaCl than CTAB. This can tentatively be attributed to a lower O_2 solubility, which would result in a more effective dedoping of PEDOT:PSS. We are currently investigating the use of oxygen radical scavenging additives (e.g., tannic acids), in the electrolyte or in the PEDOT:PSS film, to prevent PEDOT:PSS oxidation by environmental O_2.[36]

The doping/dedoping processes in PEDOT:PSS films in NaCl and CTAB were further investigated by EIS (Figure 4). The Nyquist plots obtained in NaCl consist of lines almost parallel to the imaginary impedance axis. Those obtained in CTAB are not parallel to the imaginary impedance axis, in particular at high film thickness, thus suggesting a hindered

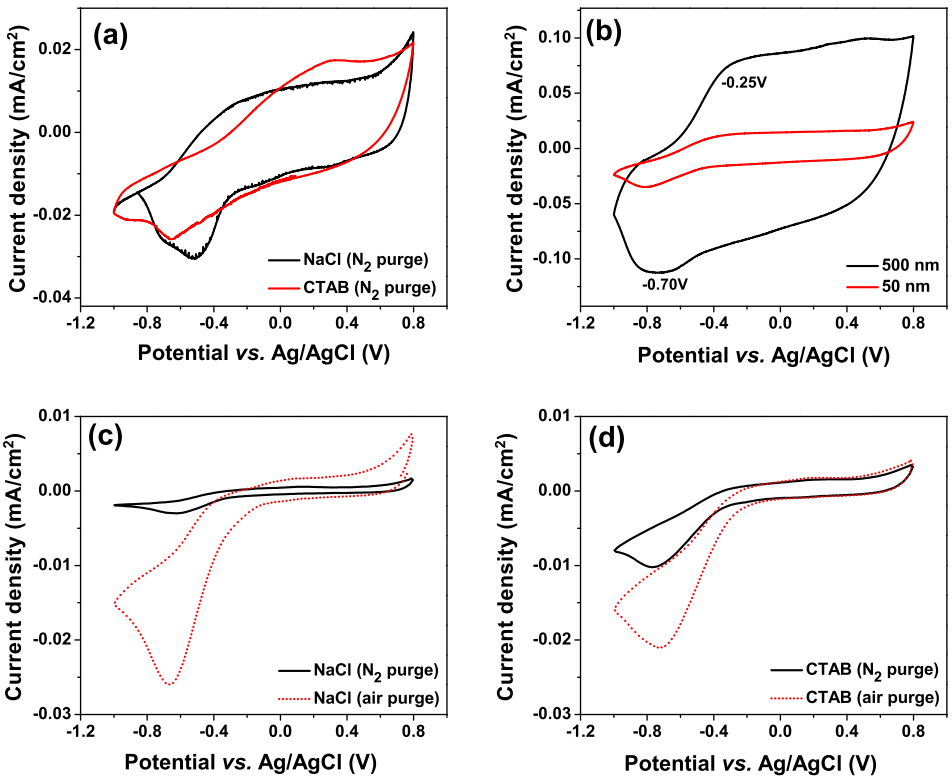

FIG. 3. Cyclic voltammetry of PEDOT:PSS films (~250 nm thickness) using 0.01M NaCl and 0.001M CTAB as the electrolytes, carried out under N_2 purging (a). Cyclic voltammetry of PEDOT:PSS films (50 nm and ~500 nm thicknesses) using 0.01M NaCl as the electrolyte, carried out under N_2 purging (b). Cyclic voltammetry of PEDOT:PSS films (~50 nm thickness) carried out under N_2 or air purging using 0.01M NaCl (c) and 0.001M CTAB (d) as the electrolyte.

TABLE II. Amount of doping charge and capacitance (absolute and volumetric values) of PEDOT:PSS films extracted from the anodic voltammetric currents at 5 mV/s in NaCl and CTAB electrolytes. The film volumes are 3.0×10^{-5} cm^3 for the thick film and 3.4×10^{-6} cm^3 for the thin film.

Electrolyte	PEDOT:PSS film thickness (nm)	Charge (C) ($\times 10^{-3}$)	Normalized charge (C/cm^3)	Capacitance (F) ($\times 10^{-3}$)	Normalized capacitance (F/cm^3)
0.01M NaCl	54 ± 10	1.52	50	1.15	38
	474 ± 90	0.25	74	0.18	54
0.001M CTAB	54 ± 10	1.44	47	1.1	41
	474 ± 90	0.23	66	0.19	55

ionic charge transport through the film. For both electrolytes, the uncompensated resistance (which includes ionic contribution from the electrolyte and electronic contribution from PEDOT:PSS) is lower for thicker films. The real component of the impedance of 500 nm-thick films at 10 kHz is ~1.9 kΩ in NaCl and ~4.9 kΩ in CTAB, while that of 50 nm-thick films is ~4.0 kΩ in NaCl and ~9.9 kΩ in CTAB. As the distance between working and reference electrodes was kept constant during all the experiments (i.e., the ionic contribution to the high-frequency real impedance for a given electrolyte remained unchanged), our results indicate that thicker films have lower electronic resistance than thin films. As expected for pseudocapacitve electrodes, the imaginary part of the impedance shows that the capacitive component of the impedance (i.e., the capacitance at the lowest frequency $C = \frac{Z_i}{2\pi f}$) increases with film thickness. In case of the NaCl electrolyte, the capacitance increases from ~0.12 mF (~35 F cm^{-3}) to ~0.69 mF (~23 F cm^{-3}) as the thickness varies from 50 nm to 500 nm. In case of CTAB, for the same thickness variation, the capacitance increases from ~0.11 mF (~32 F cm^{-3}) to ~0.42 mF (~14 F cm^{-3}). The volumetric capacitance is higher for thin films, which supports the trend observed with CV. Using the capacitance values extracted from CV (Table II) and the high frequency resistance extracted from EIS, we estimated the following time constants ($\tau = RC$) for the doping/dedoping process of PEDOT:PSS films: $\tau \sim 0.8\,s$ in NaCl and $\tau \sim 1.7\,s$ in CTAB for a 50 nm thickness and $\tau \sim 2.4\,s$ in NaCl and $\tau \sim 5.0\,s$ in CTAB for a 500 nm thickness. A similar trend was found for the time constant extracted from transient (I_{ds} vs time) OECT measurements. These results confirm that the doping/dedoping process becomes slower at higher film thicknesses and in the presence of bulky ions.

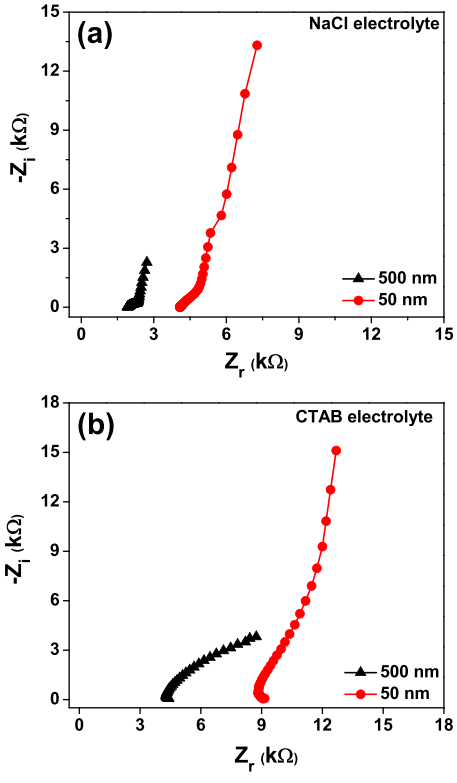

FIG. 4. Nyquist plots, obtained from EIS, of PEDOT:PSS films (thicknesses of ~500 nm and ~50 nm) in 0.01M NaCl (a) and 0.001M CTAB (b) electrolytes. PEDOT:PSS is used as working electrodes, a Pt foil as counter electrode, and Ag/AgCl as reference. The frequency range is 0.5 kHz to 10^{-4} kHz with an AC amplitude of 5 mV. The PEDOT:PSS films were doped at 0.6 V vs Ag/AgCl for 30 s prior to EIS by chronoamperometry.

In conclusion, we investigated the effect of channel thickness, electrolyte ions (NaCl and CTAB), and dissolved oxygen on the performance of OECTs based on PEDOT:PSS. We found that (i) higher ON/OFF ratios are achieved when CTAB is used as the electrolyte; (ii) thin PEDOT:PSS films have superior performance as OECT channels, in terms of current modulation, compared to their thicker counterpart, despite their lower electrical conductivity; (iii) the effect of thickness on current modulation is more pronounced when CTAB is used as the electrolyte. Using cyclic voltammetry, we detected a significant effect of dissolved O_2 on the CV current of PEDOT:PSS, particularly in the presence of a NaCl electrolyte. The dissolved oxygen might oxidize PEDOT:PSS during the electrochemical dedoping process, thus leading to a lower ON/OFF ratio. EIS revealed that the doping/dedoping process in PEDOT:PSS becomes slower at higher film thicknesses and in the presence of bulky ions.

The authors are grateful to Professor C. Santato and E. Hubis for fruitful discussions and to D. Pilon for technical support. Funding for this project was provided by an *NSERC Discovery* grant and start-up funds from Polytechnique Montréal awarded to F.C. P.K. is grateful to GRSTB for partial salary support. Z.Y. and S.Z. are grateful to NSERC for financial support through Vanier Canada Graduate Scholarships. F.S. acknowledges financial support from Alma Mater Studiorum-Università di Bologna (researcher mobility program, Italian-Canadian cooperation agreement). This work was supported by CMC Microsystems through the programs *MNT Financial Assistance* and *CMC Solutions*. This work has also benefited from the support of FRQNT

and its *Regroupement stratégique* program through a grant awarded to RQMP.

[1]M. Berggren and A. Richter-Dahlfors, Adv. Mater. **19**(20), 3201 (2007).
[2]D. A. Bernards and G. G. Malliaras, Adv. Funct. Mater. **17**(17), 3538 (2007).
[3]G. Tarabella, F. M. Mohammadi, N. Coppedè, F. Barbero, S. Iannotta, C. Santato, and F. Cicoira, Chem. Sci. **4**(4), 1395 (2013).
[4]J. M. Leger, Adv. Mater. **20**(4), 837 (2008).
[5]J. Rivnay, R. M. Owens, and G. G. Malliaras, Chem. Mater. **26**(1), 679 (2014).
[6]J. Isaksson, P. Kjall, D. Nilsson, N. D. Robinson, M. Berggren, and A. Richter-Dahlfors, Nat. Mater. **6**(9), 673 (2007).
[7]Z. T. Zhu, J. T. Mabeck, C. Zhu, N. C. Cady, C. A. Batt, and G. G. Malliaras, Chem. Commun. **2004**, 1556.
[8]M. M. de Kok, M. Buechel, S. I. E. Vulto, P. van de Weijer, E. A. Meulenkamp, S. H. P. M. de Winter, A. J. G. Mank, H. J. M. Vorstenbosch, C. H. L. Weijtens, and V. van Elsbergen, Phys. Status Solidi A **201**(6), 1342 (2004).
[9]Y. H. Kim, C. Sachse, M. L. Machala, C. May, L. Müller-Meskamp, and K. Leo, Adv. Funct. Mater. **21**(6), 1076 (2011).
[10]A. Campana, T. Cramer, D. T. Simon, M. Berggren, and F. Biscarini, Adv. Mater. **26**(23), 3874 (2014).
[11]D. J. Kim, N. E. Lee, J. S. Park, I. J. Park, J. G. Kim, and H. J. Cho, Biosens. Bioelectron. **25**(11), 2477 (2010).
[12]P. Lin and F. Yan, Adv. Mater. **24**(1), 34 (2012).
[13]S. Zhang, P. Kumar, A. S. Nouas, L. Fontaine, H. Tang, and F. Cicoira, APL Mater. **3**(1), 014911 (2015).
[14]F. Cicoira, M. Sessolo, O. Yaghmazadeh, J. A. DeFranco, S. Y. Yang, and G. G. Malliaras, Adv. Mater. **22**(9), 1012 (2010).
[15]P. C. Hütter, T. Rothländer, A. Haase, G. Trimmel, and B. Stadlober, Appl. Phys. Lett. **103**(4), 043308 (2013).
[16]O. Yaghmazadeh, F. Cicoira, D. A. Bernards, S. Y. Yang, Y. Bonnassieux, and G. G. Malliaras, J. Polym. Sci. Part B: Polym. Phys. **49**(1), 34 (2011).
[17]D. Khodagholy, J. Rivnay, M. Sessolo, M. Gurfinkel, P. Leleux, L. H. Jimison, E. Stavrinidou, T. Herve, S. Sanaur, R. M. Owens, and G. G. Malliaras, Nat. Commun. **4**, 2133 (2013).
[18]G. Tarabella, C. Santato, S. Y. Yang, S. Iannotta, G. G. Malliaras, and F. Cicoira, Appl. Phys. Lett. **97**(12), 123304 (2010).
[19]H. Tang, P. Kumar, S. Zhang, Z. Yi, G. De Crescenzo, C. Santato, F. Soavi, and F. Cicoira, ACS Appl. Mater. Interfaces **7**(1), 969 (2015).
[20]G. Tarabella, G. Nanda, M. Villani, N. Coppedè, R. Mosca, G. G. Malliaras, C. Santato, S. Iannotta, and F. Cicoira, Chem. Sci. **3**(12), 3432 (2012).
[21]G. Tarabella, A. G. Balducci, N. Coppede, S. Marasso, P. D'Angelo, S. Barbieri, M. Cocuzza, P. Colombo, F. Sonvico, R. Mosca, and S. Iannotta, Biochim. Biophys. Acta **1830**(9), 4374 (2013).
[22]S. Y. Yang, F. Cicoira, R. Byrne, F. Benito-Lopez, D. Diamond, R. M. Owens, and G. G. Malliaras, Chem. Commun. **46**(42), 7972 (2010).
[23]F. Dinelli, M. Murgia, P. Levy, M. Cavallini, F. Biscarini, and D. de Leeuw, Phys. Rev. Lett. **92**(11), 116802 (2004).
[24]J. Rivnay, P. Leleux, M. Sessolo, D. Khodagholy, T. Herve, M. Fiocchi, and G. G. Malliaras, Adv. Mater. **25**(48), 7010 (2013).
[25]J. Rivnay, P. Leleux, M. Ferro, M. Sessolo, A. Williamson, D. A. Koutsouras, D. Khodagholy, M. Ramuz, X. Strakosas, R. M. Owens, C. Benar, J-M. Badie, C. Bernard, and G. G. Malliaras, Sci. Adv. **1**(4), E1400251 (2015).
[26]S. Y. Yang, J. A. Defranco, Y. A. Sylvester, T. J. Gobert, D. J. Macaya, R. M. Owens, and G. G. Malliaras, Lab Chip **9**(5), 704 (2009).
[27]F. M. Smits, Bell Syst. Tech. J. **37**(3), 711 (1958).
[28]S. De and J. N. Coleman, MRS Bull. **36**(10), 774 (2011).
[29]V. G. Rao, C. Ghatak, S. Ghosh, R. Pramanik, S. Sarkar, S. Mandal, and N. Sarkar, J. Phys. Chem. B **115**(14), 3828 (2011).
[30]T. Johansson, L. A. A. Pettersson, and O. Inganas, Synt. Met. **129**(3), 269 (2002).
[31]B. Winther-Jensen, O. Winther-Jensen, M. Forsyth, and D. R. MacFarlane, Science **321**(5889), 671 (2008).
[32]M. Zhang, W. Yuan, B. Yao, C. Li, and G. Shi, ACS Appl. Mater. Interfaces **6**(5), 3587 (2014).
[33]R. Kerr, C. Pozo-Gonzalo, M. Forsyth, and B. Winther-Jensen, Electrochim. Acta **154**, 142 (2015).
[34]R. Kerr, C. Pozo-Gonzalo, M. Forsyth, and B. Winther-Jensen, ECS Electrochem. Lett. **2**(3), F29 (2013).
[35]K. K. Tintula, A. K. Sahu, A. Shahid, S. Pitchumani, P. Sridhar, and A. K. Shukla, J. Electrochem. Soc. **157**(11), B1679 (2010).
[36]S. Bubel, M. S. Menyo, T. E. Mates, J. H. Waite, and M. L. Chabinyc, Adv. Mater. **27**(21), 3331 (2015).